

Dye-laser photodetachment studies of Au⁻, Pt⁻, PtN^{-*}, and Ag^{-*}

H. Hotop†

Joint Institute for Laboratory Astrophysics, University of Colorado, Boulder, Colorado 80302

and

W. C. Lineberger‡

Joint Institute for Laboratory Astrophysics and Department of Chemistry, University of Colorado, Boulder, Colorado 80302

(Received 10 November 1972)

Photodetachment of Au⁻, Pt⁻, PtN^{-*}, and Ag^{-*} ions is studied in a crossed-beam experiment, in which a 2 keV negative ion beam is intersected by a pulsed tunable dye laser ($\Delta\lambda \approx 1-2 \text{ \AA}$). The threshold behavior of the photodetachment cross section σ for Au⁻ and Pt⁻ is found to agree with Wigner's Law $\sigma \propto k^{2L+1}$ (k : momentum of outgoing electron with orbital angular momentum L) over about 50 meV above threshold for this case, in which $L=1$. The electron affinity of Au is $(2.3086 \pm 0.0007) \text{ eV}$, that of Pt $(2.128 \pm 0.002) \text{ eV}$, whereas the one for Ag is $< 1.78 \text{ eV}$ and very probably $\lesssim 1.5 \text{ eV}$. The PtN^{-*} cross section exhibits sharp peaks due to single-photon processes; these features are ascribed either to autodetachment or predissociation of excited long-lived ($\tau \gtrsim 5 \times 10^{-13} \text{ sec}$) PtN^{-*} molecules; the present experiment measures the total cross section for the production of neutral atoms (or molecules) and therefore cannot distinguish the two possibilities. Further, saturation experiments are described in which the laser flux is so high as to saturate partially the photodetachment. This method is applied to the case of Pt⁻, for which the absolute cross section of an excited component Pt^{-*} in the beam is measured and thereby its fractional population is determined.

I. INTRODUCTION

In two recent papers¹ we reported on high resolution ($\Delta\lambda \approx 1 \text{ \AA}$) dye-laser photodetachment of S⁻ and Se⁻ ions and discussed in detail the behavior of the cross section near threshold. If the orbital angular momentum of the outgoing electron is L , and k its wave vector, the leading term of the energy dependence of the cross section σ_L for photodetachment of negative atomic ions is given by Wigner's law²:

$$\sigma_L = \text{const} k^{2L+1}. \quad (1)$$

The determination of any electron affinity in a photodetachment experiment, in which the goal is to determine the threshold energy E_{thr} , involves an application of (1) to the experimental data in order to extrapolate the cross section σ in the near threshold region to zero and thereby determine E_{thr} . In terms of the photon energy $h\nu$, and E_{thr} , (1) can be written as

$$\sigma_L^{2/(2L+1)} = \text{const}(h\nu - E_{\text{thr}}), \quad (2)$$

which is the form normally used to extract E_{thr} from experiment. In the case of Se⁻ ($L=0$), departures from the leading-term behavior were found as close as 5 meV above threshold.^{1b} The fact that (1) may describe σ over only a few meV above E_{thr} , urges further experimental investigations of the threshold behavior of σ , using narrow bandwidth (energy spread $< 1 \text{ meV}$) light source. This is particularly true when $L=1$, which arises whenever an s or d electron is detached, e.g., in the important case H⁻($1s^2$) or in the alkali negative ions. No high-resolution photodetachment study of the threshold behavior for $L=1$ has been reported to date. Feldmann³ has measured the photodetachment of H⁻, using about 0.03 eV resolution

(FWHM); over the first 100 meV above threshold, he applied (2) in the form

$$(Q/h\nu)^{2/3} = f(h\nu), \quad (3)$$

where Q = measured cross section {dividing Q by $h\nu$ takes out the "trivial" dependence of σ_L on $h\nu$: $\sigma_L = \text{const} h\nu k^{2L+1}$, which does not affect the leading term behavior of σ_L , however, since $h\nu = \text{const}[1 + O(k^2)]$. By extrapolating to E_{thr} in this way, Feldmann obtained 0.776 eV for the electron affinity of H with an error claimed to be $< 0.02 \text{ eV}$. The accurate theoretical value E.A.(H) = 0.75421 eV by Pekeris⁴ is just outside the experimental error limits.

Feldmann assumed that the above form of the threshold law was valid over about 100 meV above E_{thr} without being sure, however, that this assumption is valid over this rather large range. We feel that the resolution and the signal-to-noise ratio in Feldmann's experiment do not allow definite conclusions to be drawn concerning this question.

When we considered testing (1) for $L=1$ cases, we focused our interest on the noble metals, in particular Ag and Au, which, according to the literature, had electron affinities of $(2.0 \pm 0.2) \text{ eV}$ and $(2.8 \pm 0.1) \text{ eV}$ respectively, thereby providing thresholds within the energy range of our dye-laser light source. These numbers relative to iodine had been determined by Bakulina and Ionov⁵ using surface ionization. In a different surface ionization experiment Zandberg *et al.*⁶ found E.A.(Ag) = $(1.90 \pm 0.15) \text{ eV}$.

The Ag and Au atoms have $^2S_{1/2}$ ground states, and their negative ions are expected to be stable only in the 1S_0 state, the outer s shell having been filled. One therefore releases an s -electron in the photodetachment

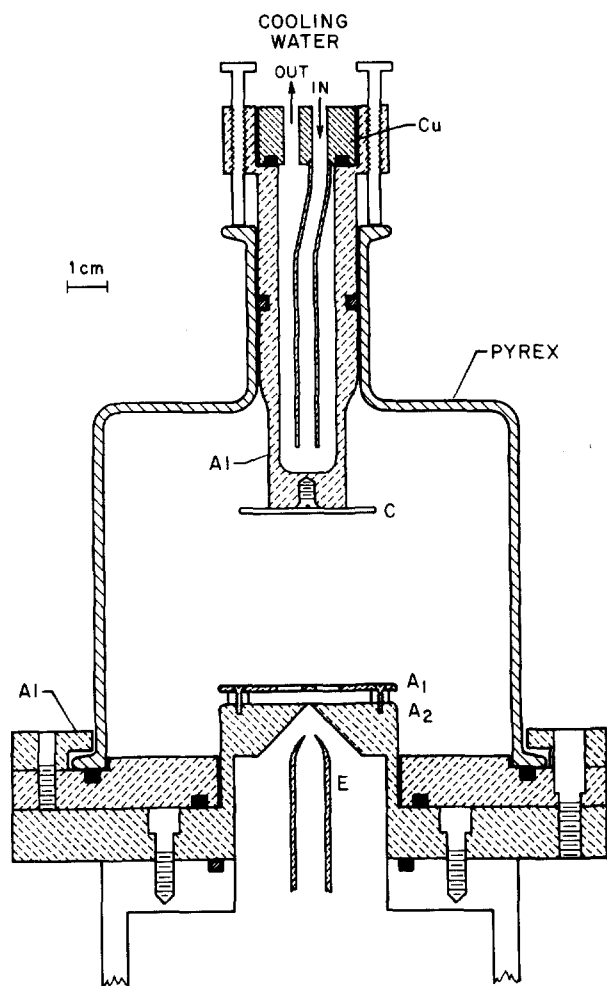


FIG. 1. Sputter ion source used in the present work for production of negative ion beams of Ag^- , Au^- , Pt^- , and PtN^- . C—noble metal cathode; A_1 , A_2 —anode plates; E—negative ion extractor. Most parts of the source are made of aluminum (Al).

process, and a p -electron wave results in the exit channel as in the case of H^- .

We started out to study photodetachment from an Ag^- beam, but found that for Ag^- we were not able to reach the threshold ($E_{\text{thr}} < 1.78$ eV), while the onset for Au^- came about 0.5 eV lower than expected. This result, besides its relevance to the surface ionization data, bears on a recent paper by Zollweg.⁷ He determined electron affinities of the three long series in the periodic table by isoelectronic extrapolation (horizontal analysis) and used the surface ionization values for Ag and Au as "benchmarks" in the second and third long period. We also report here on studies of Pt^- and of the, as it turns out, interesting species PtN^- .

In addition to the threshold studies and absolute cross section estimates some saturation experiments are described, in which the photon flux of the focused pulsed dye-laser is so high that the detachment is almost saturated. Two applications of saturation measurements are: (1) the determination of absolute

photodetachment cross sections without knowledge of either the target density or the detection efficiency of the photodetachment products, and (2) a measurement of the fractional population of excited states in the negative ion beam.

II. EXPERIMENTAL

The apparatus used for the present experiments has been described in detail in a recent paper,^{1b} and we shall focus here on the major modification made, namely the ion source for production of noble metal negative ions.

Briefly, noble metal negative ions are formed in a cold cathode discharge sputter ion source (described in detail below), extracted into a differentially pumped region and accelerated to 2 keV, mass analyzed in a 90° magnetic mass spectrometer, and crossed at right angles with the light from a pulsed (5/sec), flashlamp pumped tunable dye laser ($\Delta\lambda = 1-2$ Å; 0.5-5 mJ/pulse). The fast neutrals, resulting from the photon-negative ion interaction, are detected with an EMI multiplier, whose output charge is measured in a linear mode, giving rise to a step-like analog signal, whose step height is proportional to the neutral production signal. Gated detection is used, which discriminates strongly against noise from neutrals that are formed when negative ions lose their extra electron in collisions with the background gas.

A small fraction of the dye-laser light is coupled out by a beam splitter and measured with a photodiode. The ion beam is monitored with a Keithley electrometer. The experiment is controlled by a PDP8/L computer.

For each shot of the dye laser, the analog signals corresponding to the fast neutrals formed N , photodiode output L , and ion beam current I , are digitized, and the computer calculates an apparent cross section Q via $Q = N/LI$. At each selected wavelength, the laser is fired an appropriate number of times (typically 300), the computer sums the individual Q 's and outputs the average Q . For more details of the data taking procedure see Ref. 1.

The ion source is of rather simple construction (Fig. 1). It resembles the assembly described by Belser⁸ who used the setup for investigation of sputtering of a variety of metals. The idea is to get neutral atoms (and possibly negative ions) into the gas phase via sputtering off the cathode by bombardment with the positive ions from the discharge, and then extract negative metal ions, formed by a number of possible processes, from an appropriately designed anode.

The metal under study serves as the (cold) cathode C of the diode discharge system and is disk-shaped (diameter $d \approx 35$ mm). The anode A_1 , A_2 consists of two electrically connected parallel plates ($d \approx 40$ mm) and is the same design as in the hot cathode discharge sources used in this laboratory for the production of a variety of negative ions such as O^- , H^- , S^- , Se^- , etc.

The anode plate A_1 has a solid center with open area around it and thus offers protection from direct electron bombardment for the exit hole ($d=2$ mm) in the exit plate A_2 . Negative ions are drawn out by means of field penetration from the extractor E and originate from the plasma sheath region.

The anode-cathode distance is about 40–50 mm. The cathode is mounted on a water-cooled Al rod, which is sealed to the enclosing glass bulb by a Viton O-Ring. The dimensions of the glass bulb were large enough to prevent shorting out of the discharge via metal covered walls. The glass container was air cooled.

Typical parameters of the discharge arc were pressure ≈ 0.1 – 0.3 torr, current 10–20 mA, voltage 5 kV. Discharge carrier gases used for the present studies were various mixtures of N₂ and O₂. The more conventional use of noble gases such as Ar led to difficulties in the

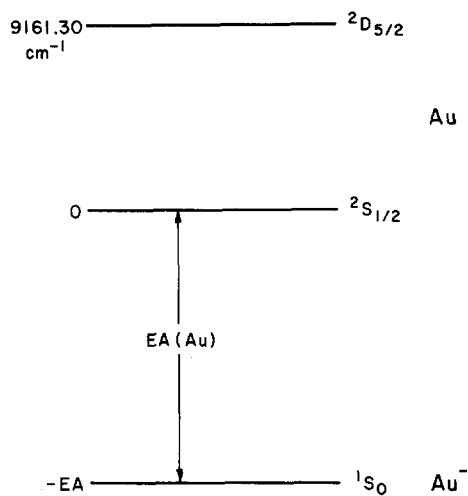


FIG. 2. Level diagram of Au and Au⁻.

ion-pump evacuated detachment region as a result of ion-pump breakdown and had to be abandoned.

We reproducibly obtained 10–20 nA of Ag⁻, Pt⁻, and Au⁻ mass-analyzed ion current (mass resolution about 30), ≈ 1 nA of PtN⁻ (with variable admixtures of PtO⁻), and typically 100–200 nA of O⁻, 30–50 nA of O₂⁻, as well as about 10–50 nA of NO⁻. The simplicity of construction and operation of this source make it an attractive means for production of stable negative ion beams of relatively unreactive metals.

III. RESULTS AND DISCUSSION

A. Au⁻

Figure 2 shows the level diagrams of Au and Au⁻. Au has a $5d^{10}6s^2$ $S_{1/2}$ ground state, the first excited state being more than 1 eV above⁹ and not accessible in the photon energy range of the described experiment. The ground state of Au⁻ should be $5d^{10}6s^1$ $1S$, with no other stable negative ion state being likely. In a measurement

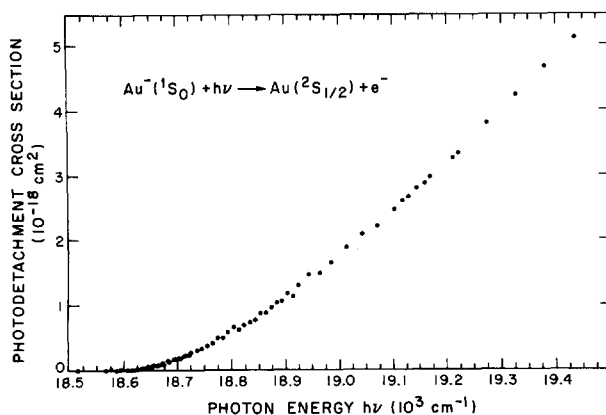


FIG. 3. Absolute cross section in units of 10^{-18} cm² for photodetachment of Au⁻ in the photon energy range 18 500–19 500 cm⁻¹ (1 eV = 8065.466 cm⁻¹).

of the photodetachment cross section, which, near threshold E_{thr} , will exhibit the p -wave behavior (3) since an s -electron is detached, the first onset will correspond to the Au⁻($1S_0$) \rightarrow Au($2S_{1/2}$) or electron affinity transitions, the transition Au⁻($1S_0$) \rightarrow Au($2D_{5/2}$) coming in more than 1 eV later.

Figure 3 shows the data obtained in the photon wave-number range 18 500–19 500 cm⁻¹ (1 eV = 8065.466 cm⁻¹).¹⁰ There is zero apparent cross section below 18620 cm⁻¹ (2.3086 eV); above that energy one finds a cross section behavior compatible with Wigner's law for p -wave electrons $\sigma \propto k^3$. This is clearly demonstrated in Fig. 4, where we plot $(Q/h\nu)^{2/3} = f(h\nu)$, according to Eq. (3) and obtain a straight line over a rather large energy range above threshold (up to about 50 meV above E_{thr}). We recall here that deviations from Wigner's law in the s -wave case Se⁻ became visible as close as 5 meV above threshold.

It is not obvious why the deviation from (1) is rather small for the p -wave case Au⁻ and rather prominent for the s -wave case Se⁻. O'Malley¹¹ has investigated the

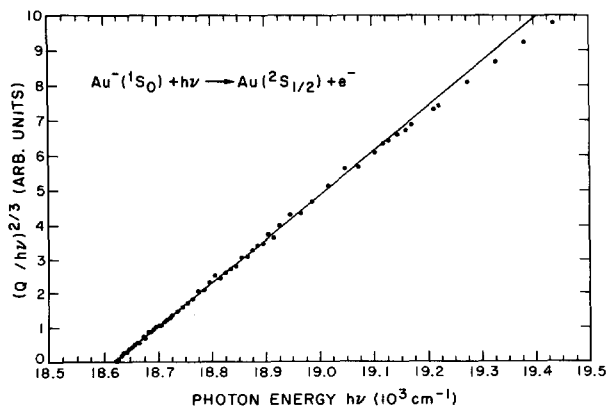


FIG. 4. Plot of $(Q/h\nu)^{2/3}$ versus photon energy $h\nu$ in the range 18 500–19 500 cm⁻¹ with Q = photodetachment cross section of Au⁻. Straight line behavior corresponds to Wigner law for photodetachment cross section near threshold.

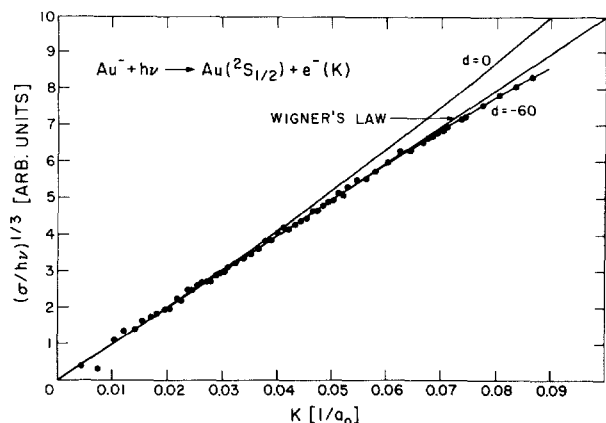


FIG. 5. Plot of $(\sigma/h\nu)^{1/3}$ versus momentum k of photodetached electron for Au^- photodetachment. Wigner law is given by straight line $(\sigma/h\nu)^{1/3} = 100k$ (ejected electron is a p wave). Points correspond to data normalized to fit Wigner's law for $k < 0.06$, where a straight line represents a very good description of the data. Also shown are threshold expressions $(\sigma/h\nu)^{1/3} = 100k \times [1 - 19.2k^2 \ln k + dk^2]$ which include correction terms to Wigner Law, the $k^2 \ln k$ term being due to electron-induced dipole interaction in the $\text{Au} + e^-$ final channel (see text). k is always measured in atomic units ($1/a_0$, $a_0 = \text{Bohr radius}$).

influence of long-range forces (besides the centrifugal potential) on the photodetachment cross section.

He found that in addition to correction terms of the form $[1 + O(k^2)]$,

$$\sigma_L = \text{const} h\nu k^{2L+1} [1 + O(k^2)],$$

which are present even for short-range potentials,¹² a correction term proportional to $k^2 \ln k$ is also present:

$$\sigma_L = \text{const} h\nu k^{2L+1}$$

$$\times \{1 - [4\alpha k^2 \ln k / a_0 (2L+3)(2L+1)(2L-1)] + O(k^2)\}, \tag{5}$$

where α and k are in atomic units and α is the dipole polarizability of final state atom. The correction term arises from the electron-induced dipole interaction in the outgoing channel. If the atom to be left in the photodetachment process has a permanent quadrupole moment [as in the case of $\text{Se}(^3P_2)$, but not in the case of $\text{Au}(^2S_{1/2})$, of course], the coefficient of $k^2 \ln k$ term is changed to include a term proportional to the square of the quadrupole moment Q (the first-order correction term, which would be proportional to Qk , was found to vanish in the angular average).¹¹

For $L=1$, the $k^2 \ln k$ term is positive, and its absolute value is five times smaller than for $L=0$ (for equal α), for which it is negative. At $k=0.04$ (electron energy 22 meV), the $L=1$ correction term is +10% for $\alpha = 72a_0^3$ [α (Au) obtained in a Hartree-Fock calculation by Fraga *et al.*¹³], whereas in the case of Se^- detachment [$L=0$, $\alpha(\text{Se}) = 30a_0^3$],¹⁴ it is -20% (ignoring the $e^- - Q$ interaction). For the $L=0$ case, the k^2 term is likely to be negative,^{1b} thus adding to the

influence of the $k^2 \ln k$ term, and apparently it is also negative for Au^- detachment, leading, however, to a partial cancellation of the $k^2 \ln k$ term due to the difference in sign, and thereby accounting for the observed behavior of only small deviations of $[\]$ from 1 in the discussed energy range.

In Fig. 5 we have plotted $(\sigma/h\nu)^{1/3}$ for the following three cases

$$\sigma = ch\nu k^3 \tag{6a}$$

$$\sigma = ch\nu k^3 [1 - 19.2k^2 \ln k] \tag{6b}$$

$$\sigma = ch\nu k^3 [1 - 19.2k^2 \ln k - 60k^2] \tag{6c}$$

together with the experimental data $(Q/h\nu)^{1/3}$ (points).

As is clearly seen, Wigner's law (6a) describes the experimental results very well up to about $k \approx 0.06a_0^{-1}$, whereas (6c) is a good fit over the entire range covered.

The coefficient c can be obtained from the absolute cross section (see Fig. 3), which was determined relative to that for O^- in a way described earlier.^{1b} At $h\nu = 19120 \text{ cm}^{-1}$ we obtained,

$$\sigma(\text{Au}^-) = 2.6 \times 10^{-18} \text{ cm}^2 \pm 30\%.$$

B. Pt⁻

The photodetachment cross section of Pt^- is expected to be more complicated than the one for Au^- as a result of the more complicated level diagram of Pt and Pt^- , which is sketched in Fig. 6.

The ground state of Pt^- is expected to be (in LS

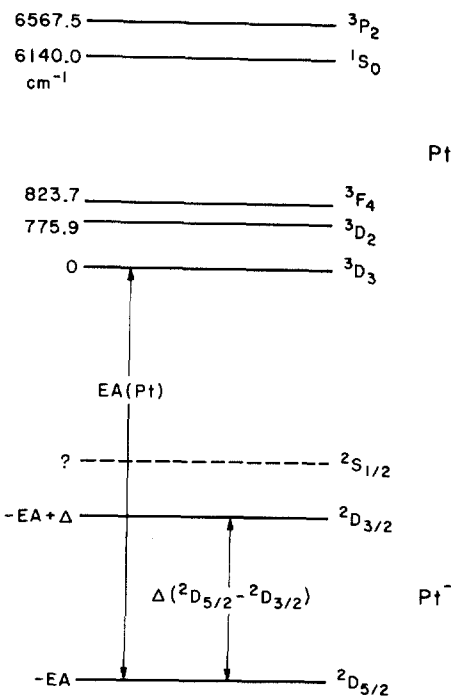


FIG. 6. Level diagram of Pt and Pt^- ; for details concerning the Pt^- levels, see text.

notation) $5d^9 6s^2 {}^2D_{5/2}$ in contrast to the $5d^{10} 6s {}^2S_{1/2}$ ground state of the isoelectronic atom. Excited negative ions Pt^{-*} may be present to some degree in the Pt⁻ ion beam: isoelectronic extrapolation of the ${}^2D_{5/2}$ - ${}^2D_{3/2}$ splitting for Pt⁻ by either use of Sommerfeld's formula or a procedure described in Ref. 1 leads to an estimate $\Delta_{5/2-3/2} \approx 10\,000\text{ cm}^{-1}$ in agreement with an estimate by Zollweg⁷; the electron affinity of Pt can be estimated to be 2.1 eV,¹⁵ using isoelectronic extrapolation based on E.A.(Au) = 2.3086 eV, which means that besides ${}^2D_{5/2}$, the ${}^2D_{3/2}$ state is also stable. Its lifetime (magnetic dipole radiation to ${}^2D_{5/2}$) is long enough (estimate: 10^{-2} sec)¹⁶ that ${}^2D_{3/2}$ Pt⁻ ions do not decay during the flight time from the ion source to the detachment chamber ($\approx 2.5 \times 10^{-5}\text{ sec}$).

Another possible excited state of Pt⁻ is the $5d^{10} 6s {}^2S_{1/2}$ configuration. Zollweg⁷ estimates that this state is about 12850 cm⁻¹ above the Pt⁻ ground state, and therefore it should also be bound. The lifetime for radiative decay of ${}^2S_{1/2}$ (to ${}^2D_{3/2,5/2}$ via electric quadrupole transition) is also estimated to be long ($> 10^{-2}\text{ sec}$).¹⁶

Figure 7 displays the experimental data, taken over the photon-energy range 15 700 cm⁻¹-19 600 cm⁻¹. One finds a rather small near constant apparent cross section Q between 15 700-17 260 cm⁻¹, slightly decreasing to higher photon energies; at 17 160 cm⁻¹, Q starts to rise exhibiting an energy dependence typical for an outgoing p -electron wave. This is shown more clearly in Fig. 8, in which $(Q_c/h\nu)^{2/3}$ is plotted versus photon energy $h\nu$, where Q_c is the apparent cross section above 17 160 cm⁻¹ after subtracting the almost constant Q below 17 160 cm⁻¹ which was extrapolated towards higher energies by a straight-line with small negative slope (determined by the region 16 500-17 100 cm⁻¹). The result obtained is very similar to the one for Au⁻ (Fig. 4); the threshold value determined from this plot is $(17\,160 \pm 16)\text{ cm}^{-1}$ or $(2.128 \pm 0.002)\text{ eV}$.

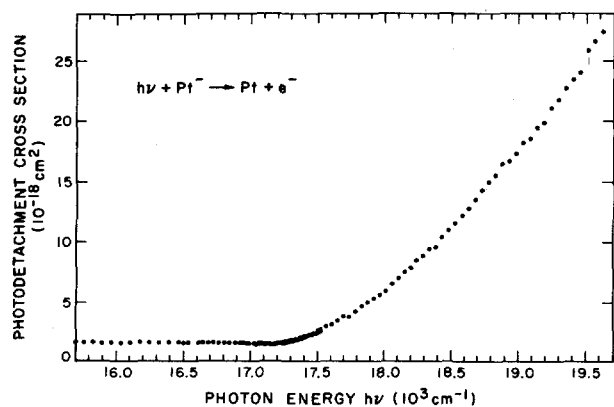


FIG. 7. Apparent absolute cross section for Pt⁻ photodetachment over photon energy range 15 700-19 600 cm⁻¹. The nearly constant cross section below 17 160 cm⁻¹ is due to detachment from excited long-lived Pt^{-*} negative ions.

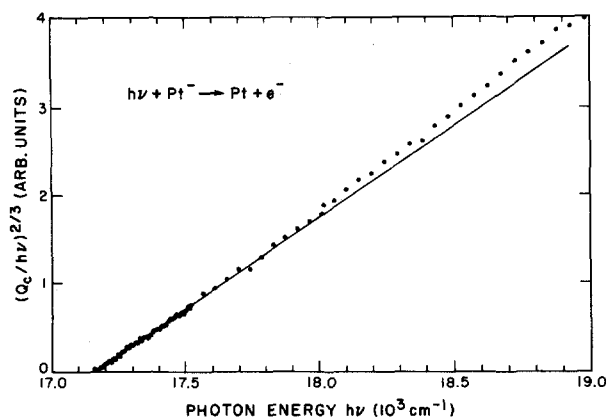


FIG. 8. Plot of $(Q_c/h\nu)^{2/3}$ versus photon energy $h\nu$ in the range 17 000-19 000 cm⁻¹; Q_c is the Pt⁻ photodetachment cross section after subtraction of the cross section already present below 17 160 cm⁻¹ which was extrapolated to $h\nu > 17\,160\text{ cm}^{-1}$ using a straight line with small negative slope, as determined from a fit to the region 16 500-17 100 cm⁻¹.

We attribute this threshold to the onset for the electron affinity transition Pt⁻(${}^2D_{5/2}$) → Pt(3D_3), in which an s electron is released, yielding the p -wave behavior observed in Fig. 8. As for Au⁻, Wigner's law appears to be a good description of the cross section over at least 50 meV above threshold. At about 18 000 cm⁻¹, 100 meV above threshold, two further channels open (3D_2 , 3F_4 , see Fig. 6). Their effect on Q_c is not very pronounced (Fig. 8). This may be partly explained by the assumption that beyond 18 000 cm⁻¹ $Q_c[\text{Pt}({}^2D_{5/2}) \rightarrow \text{Pt}({}^3D_3)]$ no longer increases as strongly as before.

The agreement of the value E.A.(Pt) = 2.128 eV with the extrapolated 2.1 eV value¹⁵ is satisfactory and confirms the above identification of the onset at 17 160 cm⁻¹. The nonzero cross section below this point very probably arises from detachment of excited Pt^{-*} ions, ${}^2D_{3/2}$ and ${}^2S_{1/2}$ being the candidates as discussed above. Since the mass resolution of our apparatus does not allow us to separate neighboring masses at $M \approx 200$ we cannot be totally sure that there is not a small PtH⁻ component in our Pt⁻ ion beam. We have been careful not to use H-containing gases for running the sputter-discharge source; only mixtures of N₂ and O₂ were used in the experiments described in this paper. The only major sources for hydrogen are thus water vapor and hydrocarbons present in the sputter source as contaminants. From the little amount of OH⁻ observed in comparison with O⁻ we conclude that PtH⁻ is, apart from the fact that the electron affinity of PtH may be higher than that for Pt⁻, unlikely to account for the cross section below 17 160 cm⁻¹.¹⁷

The behavior of the cross section between 15 700 cm⁻¹ and 17 160 cm⁻¹ is consistent with a binding energy of the corresponding state (states) of about 1-1.5 eV less than that for the ground state of Pt⁻, if one compares with the corresponding H⁻ cross section.¹⁸

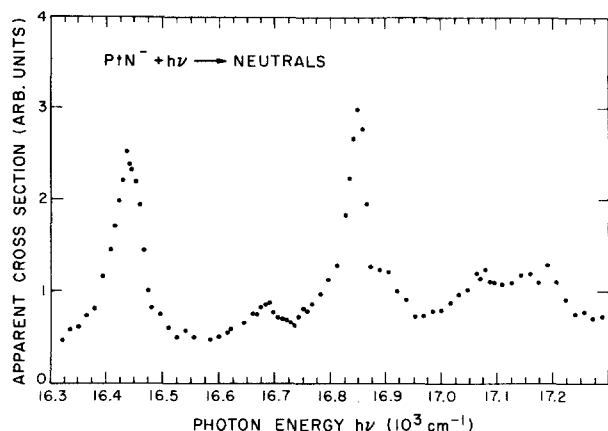


FIG. 9. Apparent cross section for the production of neutrals by photon impact on PtN^- negative ions in photon energy range 16 300–17 300 cm^{-1} . The observed cross section is due to single photon processes, as concluded from a study of the cross-section dependence on laser power.

Obviously, only p waves result near threshold for detachment from any of the discussed Pt^- states. We have determined the absolute cross section for detachment at $h\nu = 16\,900\text{ cm}^{-1}$ in a saturation experiment, described in detail below for the case of Ag^- , and obtained $\sigma(\text{Pt}^*; 16\,900\text{ cm}^{-1}) = 47 \times 10^{-18}\text{ cm}^2$ ($\pm 40\%$). Assuming that the spatial distribution of ground-state Pt^- and Pt^* in the Pt^- beam is the same, we can thus determine the fraction f_{exc} of excited Pt^* in the total beam (with current i_{tot}) via

$$f_{\text{exc}} = i(\text{Pt}^*)/i_{\text{tot}} = Q_{\text{App}}(16\,900\text{ cm}^{-1})/\sigma(16\,900\text{ cm}^{-1}), \quad (7)$$

where $Q_{\text{App}}(16\,900\text{ cm}^{-1})$ is the apparent absolute cross section at $h\nu = 16\,900\text{ cm}^{-1}$, determined by comparison with O^- . We obtain $f_{\text{exc}} = 3.6\%$. With this knowledge we can then evaluate separately the absolute cross section for detachment of ground-state Pt_{GS}^- [extrapolating $\sigma(\text{Pt}^*)$ as discussed in connection with Fig. 8]. We find

$$\sigma(\text{Pt}_{\text{GS}}^-; 18\,530\text{ cm}^{-1}) = 11 \times 10^{-18}\text{ cm}^2 \pm 30\%.$$

C. Pt N^-

In the course of our investigation of Pt^- detachment we also looked at the cross section behavior of the ion mass peak adjacent to the Pt^- peak ($M \approx 195$), centered at about $M = 209\text{--}210$. We observed rapid variations of the apparent cross section over narrow energy ranges of a few meV, which led us to study these ions in some more detail. We found that the structure is associated with the presence of N_2 in the ion source: when a mixture of CO and O_2 or pure O_2 or pure CO was tried, we were not able to see the mentioned structure, whereas it was most prominent when pure N_2 was used. We therefore concluded that the neutral production

cross section shown in Fig. 9 is associated with the PtN^- molecular ion (with a small contribution from PtO^- being possible, as far as the smooth part of the cross section is concerned; oxygen is an always present contaminant in the ion source).

Two sharp peaks at 16 440 and 16 850 cm^{-1} ($\Delta E = 51\text{ meV}$) are the prominent features in this highly structured cross section. We would like to emphasize that we measure an apparent cross section for the total production of neutrals; its interpretation as a photo-detachment cross section in this case of a molecular negative ion is not guaranteed as in the case of atomic negative ions.

We measured the dependence of the cross section on laser power at 16 850 cm^{-1} (peak) and at 16 600 cm^{-1} (valley between the two major peaks), and found that at both energies it exhibits one-photon characteristics so that an interpretation of the peaks in terms of two-photon processes proceeding via real intermediate states, as recently observed¹⁹ for C_2^- , is not possible.

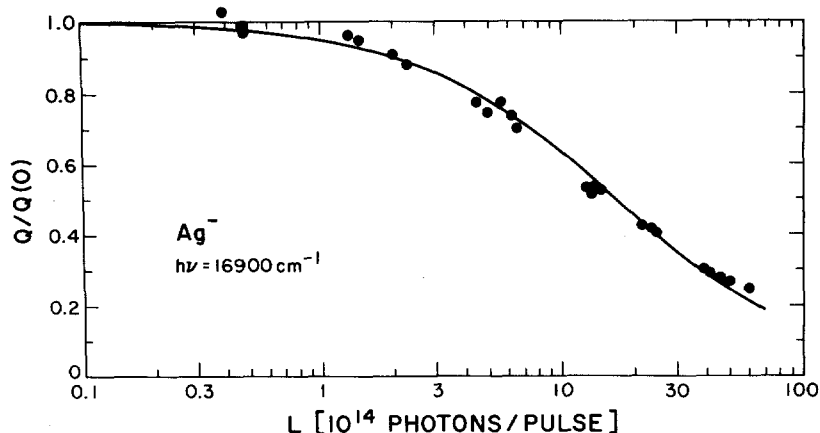
With our present knowledge two different explanations of the observed neutral production cross section appear possible:

(1) Single photon detachment of PtN^- , which proceeds via an autodetaching PtN^* excited state, located in the $\text{PtN} + e$ continuum, with a lifetime of at least a few $\times 10^{-13}\text{ sec}$ (as can be inferred from the width of the peaks).

(2) Single photon dissociation of PtN^- , in which one excited a PtN^* state from which predissociation occurs. In both cases the two observed peaks are likely to be associated with two vibrational levels of the excited PtN^* state, though it could also be that they are due to spin-orbit splitting. It is improbable that they are the result of transitions from different PtN^- vibrational levels to the same upper state; in that case the widths of the peaks should be the same and their height rather different as a consequence of lower population of higher vibrational levels in the PtN^- beam.

The electronic ground state of PtN^- may be expected to be $^1\Sigma$ as in the isoelectronic molecule PtO .²⁰ Consequently the excited state in question is most likely to be $^1\Sigma$ or $^1\Pi$ (though a $^3\Pi$ state may also have enough oscillator strength to the ground state to produce the observed features). It is interesting to note that an allowed transition in the 16 900 cm^{-1} range has been observed in the PtO molecule and interpreted as a $^1\Sigma \rightarrow ^1\Sigma$ transition.²⁰ If one assumes, based on the structure of the presumably corresponding states of PtO ,²⁰ that the rotational constant of the PtN^* state is less than that of the PtN^- ground state, then the sharp peaks in Fig. 9 are R -branch band heads.²¹ The lowest dissociation limit of PtN^- is $\text{Pt}^-(^2D) + \text{N}(^4S)$ ²²; if the PtN^- ground state is indeed $^1\Sigma$ this means that it cannot dissociate to the lowest dissociation limit. Possible limits for the $^1\Sigma$ state are $\text{Pt}^-(^2D) + \text{N}(^2D, ^2P)$

FIG. 10. Dependence of the apparent Ag⁻ photodetachment cross section at $h\nu = 16\,900\text{ cm}^{-1}$ on photon flux. $Q(0)$ corresponds to cross section obtained in the limit of zero photon flux. Solid line is calculated behavior of saturation curve for average laser spot size 0.18 mm, as explained in text. Photon flux was varied by using neutral density filters.



or Pt(³D)+N⁻(³P). If case (2) is actually responsible for what is seen in Fig. 9, it seems likely that the detected species is N(⁴S) resulting from (a possibly forbidden) predissociation of PtN^{-*}.²³ The difference in width of the two sharp peaks may be due to different lifetimes of the two levels involved; too little about the details of the levels etc. is known, however, to draw quantitative conclusions.

D. Ag⁻ Detachment and Saturation Experiment

Photodetachment from Ag⁻ ions was studied in the range 7000–5700 Å. We found that the cross section is nearly constant in the range 6200–5700 Å, and at 7000 Å it is only about 25% smaller than around 5900 Å. Our data show that the electron affinity of Ag has to be <1.78 eV, and from the shape of the observed cross section we conclude by comparison with the H⁻ photodetachment cross section,¹⁸ that E.A.(Ag) ≲ 1.5 eV.

The absolute cross section was determined relative to that for O⁻ in many different experiments with various configurations of the laser beam, as described earlier. At $h\nu = 16\,900\text{ cm}^{-1}$ (2.1 eV) it is

$$\sigma(\text{Ag}^-) = (65 \pm 10) \times 10^{-18} \text{ cm}^2,$$

with $\sigma(\text{O}^-) = 6.2 \times 10^{-18} \text{ cm}^2$ at that wavelength, as determined by Branscomb *et al.*²⁴ During these experiments care had to be taken that the photon flux was not too high, because partial saturation of the detachment can be easily obtained; we recall that the apparent cross section Q , calculated by the computer for every shot of the laser is given by

$$Q = c(N/LI), \quad (8)$$

where N is the number of neutral atoms produced by photodetachment, I is the ion current, L is the number of photons in the laser pulse, and c is a constant. N is given by

$$N = dI[1 - \exp(-L\sigma b/abrv)], \quad (9)$$

where σ = absolute photodetachment cross section, τ = duration of laser pulse, and ab = area illuminated by the

laser, b/v = time spent by the ions with velocity v in the laser beam, d = constant.

If one measures Q as a function of L , one observes a behavior as plotted in Fig. 10. This dependence was measured for Ag⁻ detachment with a focused laser beam of about 0.18 mm diameter.²⁵ For small L , Q is found to be independent of L , since then the exponent $x = L\sigma/avrv \ll 1$, and therefore $1 - \exp(-x) \approx x$ with L cancelling out. For increasing L , Q essentially behaves as $1 - e^{-x}/x$, i.e., it decreases and eventually will go to zero. It has to be noted, however, that (9) is an approximation, as discussed below.

If one estimates the exponent x for the present case one obtains [$\tau \approx 0.4 \times 10^{-6}$ sec, $v(\text{Ag}^-) \approx 6 \times 10^6$ cm/sec, $a \approx 0.02$ cm, $\sigma = 65 \times 10^{-18} \text{ cm}^2$]

$$x \approx 1.6L,$$

where L is measured in multiples of 10^{15} photons/pulse. With Rhodamine 6G as the dye, our laser system is capable of an output up to about 2×10^{16} photons/pulse, which means that the exponent can be made as large as about 30 for Ag⁻ detachment, thereby approaching saturation of detachment. We should mention that Hall *et al.*²⁶ have saturated photodetachment from H⁻ using a Q-switched ruby laser, in which case even higher numbers for x can be easily achieved.

As noted above, Eq. (9) is only an approximation to the real situation. The assumptions involved are:

- (1) laser flux is spatially uniform over the rectangular area ab ,
- (2) laser pulse is square in time,
- (3) $b/v \ll \tau$,
- (4) ion beam density is homogeneous over ab ,
- (5) ion beam velocity $v \ll c$ = speed of light.

These conditions enable one to replace the real expression for N , which contains integrals over space and time, by the simple formula (9). Whereas conditions (3) to (5) are well fulfilled for the case described above, (1) and (2) cause some complications. As for (2), it is easy to measure the time-dependence of the laser pulse;

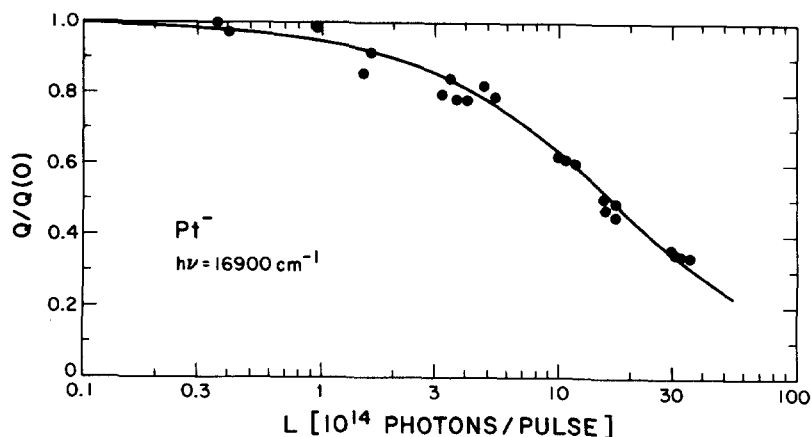


FIG. 11. Dependence of the apparent Pt^- photodetachment cross section at $h\nu = 16\,900\text{ cm}^{-1}$ (below onset for detachment from Pt^- ground state ions) on photon flux. Solid line is calculated behavior of saturation error with average laser spot size 0.18 mm and absolute cross section $47 \times 10^{-18}\text{ cm}^2$, which gives best fit to data points.

we found that in Rh 6G under typical working conditions (10^{-4} molar solution of Rh 6G in Ethanol) the time behavior was well described by the function $L(t) = (t/\tau)^{1.17} e^{-t/T}$, with t in nsec and $T = 137$ nsec. In the calculated shape of the quantity Q [Eq. (8)], we have taken this time behavior into account by carrying out the corresponding integration.

As for (1), the laser spot is not rectangular, but rather circular in the present experiment. This would not introduce major complications if the flux were spatially homogeneous; then one could insert an average a in (9), as long as for every ion passing the laser spot condition (3) is fulfilled, which is the case for spot diameters of order 0.2 mm. The laser flux is, of course, not homogeneous and its spatial intensity distribution is not easy to determine; moreover, it will vary from shot to shot. We therefore took the following approach. We measured the saturation curve as shown in Fig. 10 for Ag^- and from the knowledge of the absolute cross section for Ag^- detachment we deduced the unknown quantity in (9), a , which, of course, represents some average value. The important point is that once we have measured the saturation function for a negative ion, for which the absolute cross section is known, we can determine the (unknown) absolute cross section for other negative ions by comparing the saturation curve of the latter with the one for the former, obtained under the same experimental conditions. This does not involve any knowledge of the detection efficiency of the neutrals being formed, moreover, in the comparison, errors made in the absolute detection of the light flux cancel out. One must, of course, preserve the alignment of the system.

We applied this technique to Pt^- ions; as discussed above the nearly constant cross section below $17\,160\text{ cm}^{-1}$ (Fig. 7) can be attributed to detachment from excited Pt^{-*} ions, either $\text{Pt}^{-}(^2D_{3/2})$ or $\text{Pt}^{-}(^2S_{1/2})$ or both. These ions apparently constitute a minor fraction in the ion beam; in order to determine their absolute cross section, one does not need to know this fraction, and this makes the saturation technique very useful

indeed, and it enables one, of course, to determine that fraction once the absolute cross section is determined, as mentioned in Sec. III.B.

The saturation curve measured for Pt^- at $h\nu = 16\,900\text{ cm}^{-1}$ with the same setup used to obtain the results of Fig. 10, is shown in Fig. 11. From the comparison of Figs. 10 and 11, one gets [with $v(\text{Pt}^-) = v(\text{Ag}^-)/1.344$]

$$\sigma(\text{Pt}^{-*}) = 0.7_2 \sigma(\text{Ag}^-) = 47 \times 10^{-18}\text{ cm}^2 \pm 40\%.$$

IV. CONCLUSIONS

The major results of the present investigation are twofold: first they show that electron affinities of atoms obtained by the surface ionization method, even if measured relative to an atom for which the electron affinity is known, may give unreliable results. A more detailed discussion of this point will be given in another paper¹⁵ which will describe the measurement of the electron affinities of Cu and Ag.

Second, the data on the threshold behavior of Au^- and Pt^- detachment indicate that Wigner's law $\sigma \propto k^{2L+1}$ is a good description of the energy dependence of the cross section over about 50 meV above threshold if s electrons are detached to produce outgoing p -electron waves. One may estimate the behavior for H^- detachment near threshold in the following way: the correction term in (5), arising from the electron-induced dipole interaction, is much smaller for H^- than for Au^- or Pt^- detachment, since the polarizability of H [$\alpha(\text{H}) = 4.5a_0^3$]²⁷ is much smaller than for Au and Pt. If one assumes that the coefficient of the k^2 correction term is negative, as it is in the cases Au^- and Pt^- , one has to conclude that an extrapolation which assumes Wigner's law to be valid over the first 100 meV above threshold (as done in Ref. 3) would lead to an underestimate of E.A.(H). However, Feldmann³ obtains a value (22 ± 20) meV larger than the theoretical value,⁴ generally considered as very accurate. To remove the discrepancy one would have to assume a rather large positive coefficient of the k^2 term in (5), a result which suggests the need for further theoretical and experi-

mental investigations of the behavior of the H⁻ photo-detachment cross section near threshold.

ACKNOWLEDGMENTS

The sputter ion source was skillfully constructed by R. Weppner, D. Hendry, and C. Pelander.

* This research was supported by the Advanced Research Projects Agency of the Department of Defense and was monitored by U.S. Army Research Office-Durham, under Contract No. DAHOC4 72 C 0047.

† On leave from Fakultät für Physik, Universität Freiberg; support by the Deutsche Forschungsgemeinschaft is gratefully acknowledged.

‡ Alfred P. Sloan Foundation Fellow, 1972-1974.

¹ (a) W. C. Lineberger and B. W. Woodward, *Phys. Rev. Lett.* **25**, 424 (1970). (b) H. Hotop, T. A. Patterson, and W. C. Lineberger (unpublished).

² E. P. Wigner, *Phys. Rev.* **73**, 1002 (1948).

³ D. Feldmann, *Z. Naturf.* **25a**, 621 (1970).

⁴ C. L. Pekeris, *Phys. Rev.* **112**, 1649 (1958); *Phys. Rev.* **126**, 1470 (1962). Pekeris finds: E.A.(H) = 6083.09 cm⁻¹; using the conversion factor 8065.465 cm⁻¹ ≅ 1 eV¹⁰ one obtains: E.A.(H) = 0.75421 eV.

⁵ I. N. Bakulina and N. I. Ionov, *Sov. Phys. Dokl.* [Engl. transl.] **9**, 217 (1964).

⁶ E. Ya. Zandberg and V. I. Paleev, *Sov. Phys. Dokl.* [Engl. transl.] **15**, 52 (1970).

⁷ R. J. Zollweg, *J. Chem. Phys.* **50**, 4251 (1969).

⁸ R. B. Belsler and W. H. Hicklin, *Rev. Sci. Instr.* **27**, 293 (1956).

⁹ C. E. Moore, "Atomic Energy Levels," NBS Circular 467 (1948).

¹⁰ B. N. Taylor, W. H. Parker, and D. N. Langenberg, *Rev. Mod. Phys.* **41**, 375 (1969).

¹¹ T. F. O'Malley, *Phys. Rev.* **137**, A1668 (1965).

¹² L. M. Branscomb, D. S. Burch, S. J. Smith, and S. Geltman, *Phys. Rev.* **111**, 504 (1958).

¹³ J. Thorhallsson, C. Fisk, and S. Fraga, *J. Chem. Phys.* **49**, 1987 (1968).

¹⁴ J. Thorhallsson, C. Fisk, and S. Fraga, *Theor. Chim. Acta.* **10**, 388 (1968).

¹⁵ H. Hotop, R. A. Bennett, and W. C. Lineberger, *J. Chem. Phys.* **58**, 2373 (1973), preceding paper.

¹⁶ R. H. Garstang, *J. Res. Nat. Bur. Std.* **68A**, 61 (1964); R. H. Garstang (private communication).

¹⁷ In the case of Ag⁻ and Au⁻, it is not clear if AgH⁻ and AuH⁻ are stable negative ions at all. The electron energy spectrum obtained by detachment from an Ag⁻ beam (prepared under the same conditions as described in this paper) with an Ar ion laser (4880 Å)¹⁵ showed no trace of other transitions than the one expected, namely Ag⁻(¹S₀) → Ag(²S_{1/2}). We therefore conclude that AgH⁻ (and similarly AuH⁻), if in the beam at all, presents no problem.

¹⁸ L. M. Branscomb, discussion of H⁻ photodetachment cross section in *Atomic and Molecular Processes* (Academic, New York, 1962).

¹⁹ W. C. Lineberger and T. A. Patterson, *Chem. Phys. Lett.* **13**, 40 (1972).

²⁰ B. N. Rosen (ed.), *Spectroscopic Data* (Pergamon, Oxford, 1970).

²¹ The sharp drop at the high-energy side of the peaks is consistent with this statement.

²² The electron affinity of N(⁴S) is very small, if positive at all; see B. Steiner, in *Case Studies in Atomic Physics II*, edited by E. W. McDaniel and M. R. C. McDowell (North Holland, Amsterdam, 1972), pp. 483-545.

²³ N atoms arising from dissociation of 2-keV PtN⁻ will have rather low kinetic energy in the laboratory-system, of order 150 eV, and the probability for secondary electron emission at the multiplier cathode by impact of such low energy N atoms will be rather small, but not necessarily much less than that for PtN molecules with 2 keV kinetic energy.

²⁴ L. M. Branscomb, S. J. Smith, and G. Tisone, *J. Chem. Phys.* **43**, 2906 (1965).

²⁵ The variation of the laser flux was accomplished by use of suitable neutral density filters; pulse to pulse variations in *L* were <20% mostly no more than 10%.

²⁶ J. L. Hall, E. J. Robinson, and L. M. Branscomb, *Phys. Rev. Lett.* **14**, 1013 (1965).

²⁷ See for instance, G. Wentzel, *Z. Physik* **38**, 518 (1926); a table of atomic polarizabilities is provided by R. R. Teachout and R. T. Pack, *At. Data* **3**, 195 (1971).